# A Review Study on the Modeling and Simulation of Solar Tower Power Plants

Samir Benammar*

*Laboratoire Energétique – Mécanique & Ingénieries (LEMI), Université M'Hamed Bougara de Boumerdes, Boumerdes, Algeria*

**Abstract:** Much attention has been paid to concentrating solar power technologies (CSP) in the last two decades. Among the CSP that have been developed so far are the parabolic trough, the parabolic dish, the Fresnel collectors and the solar tower. However, the most widely used of these technologies is the solar tower power plant (STPP). This review aims to summarize the state-of-the-art modeling approaches used to simulate the performances and the reliability of the STPP. The review includes the different analytical and numerical models used in literature to predict the thermal efficiency of these STPP. A general description and comparison of different CSP technologies are first provided. An overview of STPP technology, current status and a presentation of the major components including the heliostat field and the solar receiver are then highlighted. The different research works, developed on the modeling and simulation of the STPP performances and reliability, are also investigated in this review. In summary, this work presents a comprehensive review of the existing numerical and analytical models and could serve as a guideline to develop new models for future trends in solar tower power plants.

## 1. INTRODUCTION

Industrial development such as the increasing number of vehicles and the increase in domestic equipment led to a significant growth in energy demand. This growth in demand was mainly covered by the use of fossil energy sources [1-3]. Unfortunately, these energy sources are not only polluting but also suffer from the limited nature of their resources. Furthermore, the use of hydrocarbons emits a very important quantity of $CO_2$ to the atmosphere.

To address this concern, a new source of energy has to be found. Renewable energy sources are excellent alternatives. They are abundantly available and unlimited. The development and exploitation of renewable energy are then essential [4].

There is at the world level an intensive activity to develop the renewable technology. To this end many projects and road maps have been devised [5-7].

Renewable energy sources are expected to become economically competitive as their costs already have fallen significantly compared with conventional energy sources in the medium term, especially if the massive subsidies to nuclear and fossil forms of energy are phased out [8].

*Address correspondence to this author at the Laboratoire Energétique – Mécanique & Ingénieries (LEMI), Université M'Hamed Bougara de Boumerdes, Boumerdes, Algeria; Tel: +213550924577;
E-mail: s.benammar@univ-boumerdes.dz; sa.benammar@gmail.com

Renewable Energies Come in Seven Forms:

***- Geothermal Energy***

Geothermal is energy available as heat emitted from within the earth, usually in the form of hot water or steam. Geothermal heat has two sources: the original heat produced from the formation of the earth by gravitational collapse and the heat produced by the radioactive decay of various isotopes. Geothermal is another promising renewable energy resource. The potential is estimated at 460 GWh/year.

***- Wind Energy***

Wind is generated by atmospheric pressure differences, driven by solar power. Wind power is broken up into two main categories, onshore wind power and offshore wind power. The main difference between the onshore and offshore systems is the foundations. Wind energy has in recent years attracted a lot of attention worldwide and it is on its way to becoming a serious contender to conventional energy resources.

***- Hydropower Energy***

Hydropower is the extraction of energy from falling water (from a higher to a lower altitude) when it is made to pass through an energy conversion device, such as a water turbine or a water wheel. A water turbine converts the energy of water into mechanical energy, which in turn is often converted into electrical energy by means of a generator.

E-ISSN: 2410-2199/20 

***- Biomass Energy***

Biomass energy is a generic term applied to energy production from organic material broken down into two broad categories [9]:

- **Woody biomass**. Forestry timbre, residues and co-products, other woody material including thining and cleaning from woodlands (known as forestry arisings), untreated wood products, energy crops such as willow, short rotation coppice (SRC), and miscanthus (elephant grass).
- **Non-woody biomass**. Animal wastes, industrial and biodegradable municipal products from food processing and high-energy crops such as rape, sugarcane, and corn.

***- Ocean Energy***

The energy of the ocean can be used in three basic ways [10]:

- Use the ocean's waves (wave energy conversion);
- Use the ocean high and low tides (tidal energy conversion);
- Use temperature differences in the water (ocean thermal energy conversion).

***- Hydrogen Energy***

Hydrogen is the most abundant element on earth; however, less than 1% is present as molecular hydrogen gas $H_2$; the overwhelming part is chemically bound as $H_2O$ in water and some is bound to liquid or gaseous hydrocarbons [8]. The ideal intermediary energy carrier should be storable, transportable, pollution free, independent of primary resources, renewable, and applicable in many ways [8]. These properties may be met by hydrogen when produced electrolytically using solar radiation, and hence, such a combination is referred to as the solar-hydrogen process [11].

***- Solar Energy***

Solar energy is a source, which can be exploited in two main ways to generate power: direct conversion into electric energy using photovoltaic panels and by means of a thermodynamic cycle [12]. Photovoltaics (PV) are a form of solar power where sunlight is directly generated into electricity [13]. PV cells are commonly made from semiconducting materials including silicon, copper, and cadmium. Concentrated solar power (CSP) or concentrating solar power systems uses the sunlight to create high temperatures (generally between 400 °C and 1000 °C) that will be used to produce electricity or heat [14].

Among the solar technologies under consideration, concentrating solar technologies (CSP) have the greatest potential for commercial electrical power generation [15] and they have successfully demonstrated their capability of producing high-temperature steam to power the conventional Rankine cycle for electricity generation [4,16,17]. These technologies are based on collectors which concentrate sunlight to produce steam for driving electrical generators [18]. The main technologies used in CSP plants are the parabolic trough collectors, Fresnel mirrors, dishes and finally power towers [19, 20]. Of these technologies, the parabolic trough and the solar tower technologies have reached the commercial stage.

There has been an increasing interest in solar tower technology over the last decade. In general, the previous research studies can be grouped into three different types. The first group focuses mainly on the modeling and simulation of solar tower power plants (STPP) performances [21-26]. In these studies, the main objective was to calculate the power output and the efficiency of the whole system (STPP). The second group, on the other hand, has concentrated their effort on the modeling and simulation STPP design and characteristics [27-35]. They have been interested in the development of only the principle components of STPP, such as heliostats and receivers. Finally, the third group was based in its research on the reliability of different parts of STPP [36-44].

In this paper, a general review on the modeling and simulation of STPP reliability and performances, has been provided. The aim of this study is to summary and emphasize the different previous works and ideas in this field. In the present review, an outline and brief description, including fundamentals of the different concentrated solar power (CSP) technologies, are presented. A comparison between these different CSP technologies, taking into account the relative cost, the land occupancy, the capacity and the efficiency, is also provided. Then, detailed description of solar tower power plants (STPP), including the major STPP parts such as the collector and the receiver subsystems, is introduced.

## 2. CONCENTRATING SOLAR POWER (CSP) TECHNOLOGIES

Potential concentrated solar power (CSP) sites around the world are identified using the global distri-

bution of direct normal irradiance [45]. In the sunniest countries, the area of the planet with more solar radiation, called “Sun Belt” (North Africa, the Middle East, Mediterranean, California, Arizona, Nevada, New Mexico etc.) which have vast areas with particularly high solar radiation and well suited to large amounts of solar systems [46].

Solar thermal power plants with optical concentration technologies are important candidates for providing the bulk solar electricity needed within the next few decades. Four concentrating solar power technologies are today represented at pilot and demonstration-scale [47-49]: parabolic trough collectors, linear Fresnel reflector systems, power towers or central receiver systems, and dish/engine systems. All the existing pilot plants mimic parabolic geometries with large mirror areas and work under real operating conditions. Central receiver systems are usually selected since they have better perspectives for scale-up.

CSP plants concentrate direct solar radiation to heat a fluid (normally called the heat transfer fluid or HTF) and produce steam (or vapor of another working fluid). The working fluid runs an engine (steam turbine, Stirling engine, etc.) connected to a generator, producing electricity. Four alternative configurations of the concentrators are shown in Figure **1**.

### 2.1. Parabolic Trough

The parabolic trough system is by far the most commercially matured of the three technologies [50]. It focuses the sunlight on a glass-encapsulated tube running along the focal line of the collector. The tube carries heat absorbing liquid, usually oil, which in turn, heats water to generate steam [46, 51, 52].

### 2.2. Central Receiver

In the central receiver system, an array of mirrors field focusses the sunlight on the central receiver mounted on a tower. To focus the sunlight on the central receiver at all times, each heliostat is mounted on the dual-axis sun tracker to seek position in the sky that is midway between the receiver and the sun. Compared to the parabolic trough, this technology produces higher concentration, and hence, higher temperature working medium, usually a salt. Consequently, it yields higher Carnot efficiency, and is well suited for utility scale power plants in tens or hundreds of megawatt capacity [51-54].

### 2.3. Parabolic Dish

The parabolic dish tracks the sun to focus sunlight, which drives a Stirling heat engine-generator unit. This technology has applications in relatively small capacity

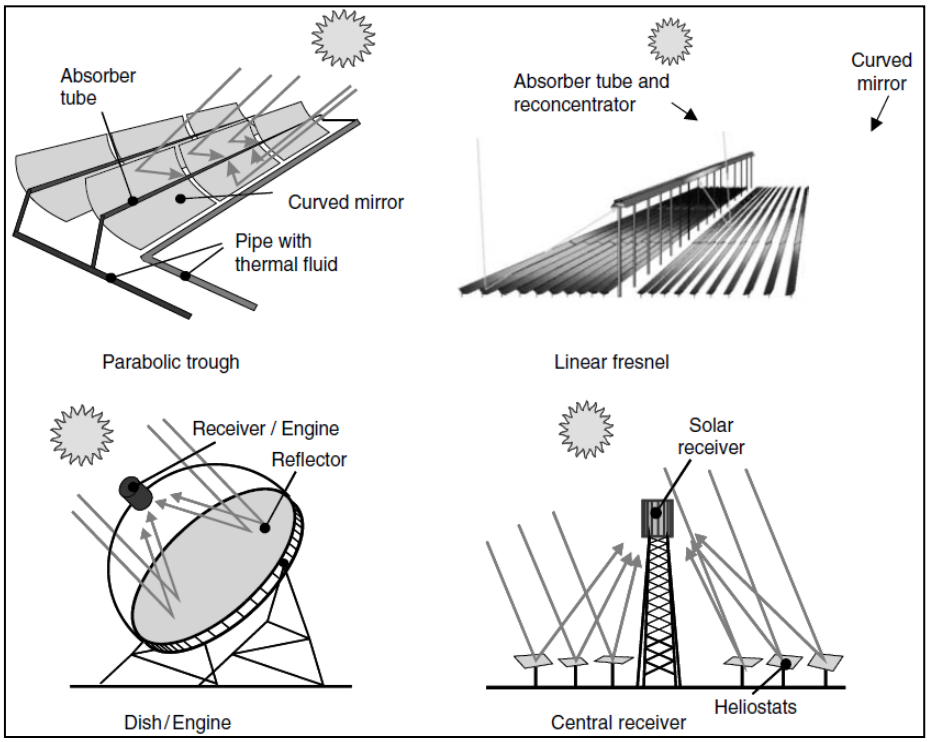


**Figure 1**: Alternative thermal energy collection technologies [45].

(tens of kW) due to the size of available engines and wind loads on the dish collectors. Because of their small size, it is more modular than other solar thermal power systems, and can be assembled in a few hundred kW to few MW capacities [18, 52, 55].

### 2.4. Fresnel Reflectors

Solar thermal power plants with Fresnel reflectors are composed of flat or slightly curved Fresnel reflectors, receivers of the concentrated sun irradiation, cylindrical-parabolic reflector, steam turbine and generator of the electrical energy. During the day Fresnel reflectors are automatically directed toward the Sun and they reflect sun irradiation toward cylindrical-parabolic reflector in whose focus there is a receiver in the shape of long tubes with running water. Under the influence of the reflected sun irradiation water in receiving tubes evaporates and under pressure runs into the steam turbine that starts generator of the electrical energy [56, 57].

In addition to these four CSP technologies, a recent technology called concentrated solar thermo-electrics is described elsewhere. As well as with photovoltaic systems, direct conversion of solar energy into electricity can also be achieved with concentrated solar thermo-electric technology.

### 2.5. Comparison of CSP Technologies

A comparative study of the various CSP technologies discussed has been presented in Table **1**. The different parameters on which we have based to compare the various CSP technologies are as flows:

- **Capital cost**: the cost related to the development of the solar tower and parabolic dish is higher than the cost of parabolic trough and Fresnel reflectors. For example, the capital of solar tower and parabolic dish is estimated by more than 4000 Dollars / kW and less than this value for the other CSP technologies (parabolic trough and Fresnel reflector).
- **Land occupancy**: The land used by parabolic trough is very large then that used by Fresnel reflectors and solar towers. A small area is used for parabolic dish. A numerical values, given by [46], indicated that the land surface required by solar tower and parabolic dish is between 8 and 12 $m^2$ for MWh/year and between 4 and 6 and 6 and 8 $m^2$ for MWh/year for Fresnel reflector and parabolic trough, respectively.
- **Capacity**: the power generation capacities range for solar tower, parabolic trough and Fresnel reflectors is from 10 to 200 MW and lower capacities are generated by parabolic dish (from 0.01 to 0.4 MW).
- **Efficiency**: solar tower and parabolic dish present high efficiency; it is about 20-35% and 25-30% for solar tower and parabolic dish respectively. In the other hand, low efficiencies are noted for Fresnel reflector (8-10%) and parabolic trough (15%).
- **Operations and maintenance cost**: O&M cost for parabolic dish is very high; it is estimated about 0.21 Dollars / kWhe. In the other hand, Fresnel reflector technology represents the lowest O&M cost. However, it reaches 0.02 Dollars / kWhe for parabolic trough and 0.034 Dollars / kWhe for solar tower technologies.
- **Operating temperature range**: the solar tower concentrator and parabolic dish concentrator work with high temperatures. The operating temperature in the solar tower is between 300 $^oC$ and 1000 $^oC$ and from 120 $^oC$ to 1500 $^oC$ for parabolic dish. Lower temperature used by the other CSP categories (parabolic trough and Fresnel reflectors); the operating temperature ranges for parabolic dish and Fresnel reflectors are respectively 20-400 $^oC$ and 50-300 $^oC$ [58].

The Table **1** below summarizes the main advantages and disadvantages of the different CSP technologies.

## 3. SOLAR TOWER POWER PLANT

As shown in Figure **2**, solar tower power plants use hundreds to thousands of large, sun-tracking flat heliostats (mirrors) to concentrate sunlight onto a receiver placed on top of a tall tower. The tower height would be proportional to the energy production of the plant [61]. Computer controlled heliostats track the sun and reflect the sunlight to the receiver. The complete group of heliostats is called the collector field. Depending on the configuration of the receiver, there are two main collector field lay outs. The collector field may surround the tower or it may be located only on one side of the tower. For a one-side lay out, the field lies north of the tower for a site located in the northern earth hemisphere; it lies south of the tower for a site located in the southern earth hemisphere. A power tower system needs preferably relatively flat terrain, with a slope of one to two percent at most [62].

**Table 1: Comparison of CSP Technologies (Advantages and Disadvantages)**

| System | Advantages | Disadvantages |
|---|---|---|
| **Central receiver** | - Thermal storage capability enables high capacity factors<br>- Relatively high efficiency<br>- Usable as intermediate or near baseload<br>- Utility familiarity with Ranking cycle power generation | - Very large system required for good economy ($>$ 30-50 $MW_e$) needed large capital investment<br>- Low density collection field – large land area<br>- Higher O&M than photovoltaics |
| **Dish** | - Highest efficiency [59, 60]<br>- Possible small modules (25 $kW_e$)<br>- Low capital investment<br>- Possible Remote unattended sitting | - Currently uneconomical storage capability (batteries)<br>- Limited to peaking applications (utility)<br>- Higher O&M than photovoltaics |
| **Parabolic trough** | - Small modular system<br>- Lowest concentrator system cost /collector area<br>- Higher density collector field | - Single axis tracking and lower operating temperature give lower efficiency than dish or central receiver<br>- High thermal losses from interconnecting piping<br>- Higher O&M than photovoltaics |
| **Fresnel reflector** | - Lower specific costs as well as a simple structure and maintenance. | - Single axis tracking and lower operating temperature give lower efficiency than dish or central receiver<br>- Lower concentrations than parabolic trough collectors. |

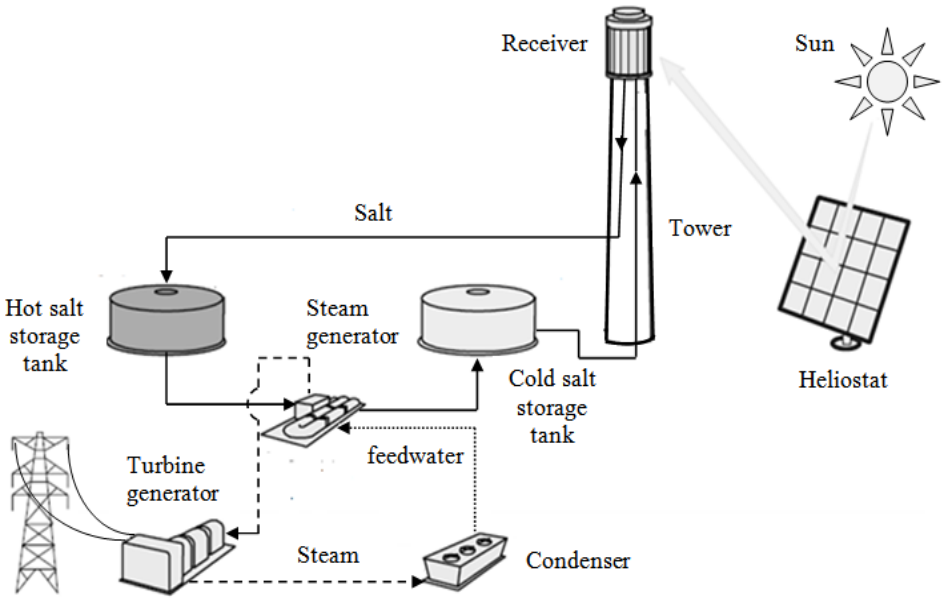


**Figure 2:** Schematic of hypothetical molten-salt central receiver system with thermal storage.

Three main central receiver designs, regarding the heat transfer fluid, have been studied until now: Solid particle receivers, gas receivers and liquid receivers. This last category (liquid receivers) is most used.

In the liquid receiver, the collected solar radiation is converted to heat in a receiver fluid such as water/ steam, liquid sodium, or molten nitrate salt flowing through small receiver tubes. If water/steam is the receiver fluid, the steam may be sent directly to the turbine generator. If one of the other receiver fluids is used, the energy in the fluid must be transferred to water/steam by means of heat exchangers before being used to generate electricity in the turbine generator.

Molten salt is the most used fluid not only as heat transfer fluid but also as storage fluid. Power tower systems would use molten salt primarily because of its superior heat-transfer and energy-storage capabilities. Molten salt is typically a mixture of sodium nitrate, potassium nitrate, calcium nitrate and/or lithium nitrate. Thermophysical properties of the most widely used molten salt mixtures are shown in Table **2**. The molten

**Table 2: Summary of Thermophysical Properties of the Most Popular Molten Salts [64, 65]**

| Molten Salt | Composition (%) | Melting Point (°C) | Thermal Stability (°C) | Heat Capacity (J/g K) | Density (kg/L) |
|---|---|---|---|---|---|
| $NaNO_3$ - $KNO_3$ | 60 %, 40% | 221.4 | 588.51 | 1.498 | 1.7 |
| $NaNO_2$ - $NaNO_3$ - $KNO_3$ | 40%, 7%, 53% | 142.24 | 630.97 | 1.439 | 1.87 |
| $Ca(NO_3)_2$ - $NaNO_3$ - $KNO_3$ | 48%, 7%, 45% | 130.61 | 554.39 | 1.272 | 1.89 |
| $Li NO_3$ - $NaNO_3$ - $KNO_3$ | 20%, 28%, 52% | 130.15 | 600.05 | 1.091 | 1.86 |

salt can be stored at different temperatures in a storage tank for use on cloudy days or after the sun has set. Also, a power tower, using molten salt rather than another type of HTF, can operate at a much higher temperature range which can improve the efficiency of the steam turbine generator (e.g., from 37.6% to 40%). The marginal cost of collecting and storing this energy is less than the cost of increasing turbine size to match the peak thermal output. Determination of the optimum storage size to fulfill the energy dispatch requirements of a particular application is a part of the central receiver design process [63].

### 3.1. Collector Subsystem

The collector subsystem for a solar central receiver has as its basic function the interception, redirection, and concentration of direct solar radiation to the receiver subsystem. The collector subsystem consists of a field of tracking mirrors, called heliostats, and a tracking control system to maintain continuous focus of the direct solar radiation on the receiver while energy is being collected. When energy is not being collected, the controls must prevent the reflected energy from damaging the receiver, tower, or other structures, or from creating an unsafe condition in the airspace around the plant [63].

#### *3.1.1. Collector Field Configuration*

Two field configurations have been developed [45, 63]: north and surround. In a surround field configuration, heliostats are arranged around a centrally located tower. The tower is usually located to the south of center to optimize field efficiency. In a north field configuration (or for plants located in the southern hemisphere, a south field configuration), all heliostats are arranged on the north side of the tower. Representative collector fields which have been developed as a result of such trade studies are shown in Figure **3** for surround and north-side fields, respectively. Selection between a north or surround field configuration is a function of the receiver configuration.

#### *3.1.2. Collector field Performance*

The performance of the heliostat field is defined in terms of the optical efficiency, which is equal to the ratio of the net power intercepted by the receiver to the product of the direct insolation times the total mirror area. The optical efficiency includes the cosine effect, shadowing, blocking, mirror reflectivity, atmospheric transmission, and receiver spillage. The different optical loss factors are well explained by [26]. The net efficiency for producing electricity includes receiver efficiency and thermal-to-electric conversion efficiency.

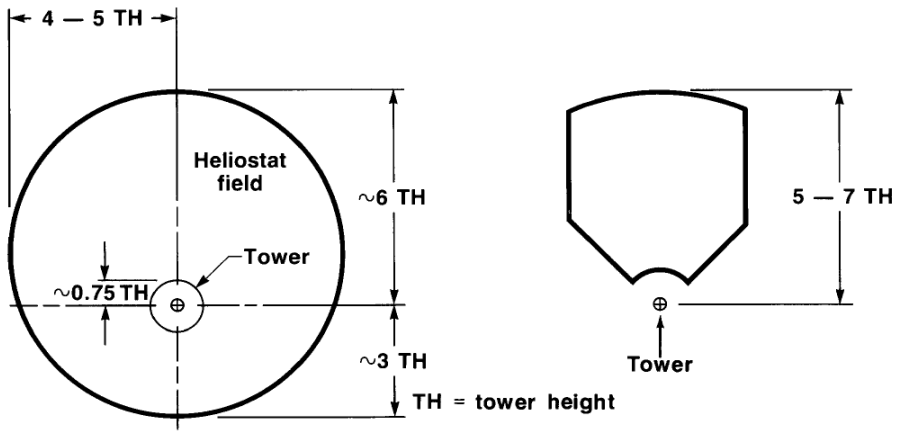


**Figure 3**: North and surround heliostat field configurations [63].

#### *3.1.3. Heliostat Layout*

The local heliostat density at any point within the collector field is determined through a trade-off of cost and performance parameters influencing that portion of the field. This trade-off considers the cost of heliostats, land, and interconnecting wiring. Clearly as heliostats are packed closer together, blocking and shadowing penalties increase, but related costs for land and wiring decrease [66].

As a design option within the collector field, alternate heliostat arrangements are possible. The two arrangements receiving the most study to date are the "cornfield" and the radial stagger arrangements. In the cornfield arrangement, heliostats are laid out along straight lines with uniform rectangular spacing being maintained throughout the section.

#### *3.1.4. Wiring*

Collector field wiring represents a significant factor in the analysis of heliostat spacing. The two wiring networks involved are the alternating current power system and the control system wiring. In each case, direct buried cable is essential for any type of cost-effective design.

#### *3.1.5. Shape*

The general outline (shape) of these fields represents a contour of constant cost per unit energy collected. In general, this reflects a tradeoff between poorer performance of close-in heliostats on the south, east, and west sides and higher performance north side heliostats. The north side heliostats, however, suffer from atmospheric losses because of the long path lengths for the reflected beams which reduce interception by the receiver [66].

The annual performance on the heliostat's position relative to the tower depends on the optimal north and surround field designs shown in Figure **3**. The observed shapes result from two effects. First, at a given radial distance, performance increases as the heliostat moves from south to north of the tower because the cosine effect is much better in the north part of the field. Second, the performance decreases in any direction as the radial distance of the heliostat increases. This decrease is caused by an increase in atmospheric attenuation and spillage losses.

The density of heliostats, chosen to minimize blocking, is greatest at the inner boundary and decreases with increasing radial distance from the tower. The average ratio of mirror area to land area is typically 0.20 to 0.25. The shape of the heliostat field remains relatively constant over a wide range of power levels [67].

#### *3.1.6. Heliostat Description*

The heliostat is the main element of the collector subsystem. A dictionary definition of a heliostat is "a mirror mounted on an axis moved by clockwork, by which a sunbeam is steadily reflected to one spot". The heliostat itself is the least dependent central receiver system component on overall system considerations; that is, unique heliostat designs are not required for each type of receiver heat transport fluid, receiver configuration, or end use application of thermal energy. This independence permits design emphasis to be placed on mass production as a means of reducing the unit cost of the heliostat, recognizing that the collector system represents a major portion of the overall system cost. There are three main types of heliostats characterized by the type of mirror module and/or structural arrangement. Glass/metal heliostats have silvered glass as the reflecting surface and a relatively stiff structure to support the mirrors and withstand wind loads. Membrane heliostats have a stressed membrane supporting a reflecting film. In a third option, the entire heliostat, either glass or membrane, may be enclosed in a pressurized bubble. Heliostats enclosed by a bubble are subjected to virtually no wind loads, and thus can have a lighter (and potentially lower cost) support structure. However, if the heliostat is enclosed in a bubble, the energy must pass through the bubble material twice, and in so doing can be absorbed and scattered by the bubble material or by dirt on the bubble material. Stressed membrane heliostats offer the potential of lower cost through reduced material cost [67].

### 3.2. Receiver Subsystem

#### *3.2.1. Olid Particle Receivers*

Initially, the solid particle receivers (SPRs) have been studied in the early 1980s in order to create a direct absorption central receiver which is able to interface with high temperature (> 900 $^{o}$C) electric power and chemical production cycles [68-70]. SPRs have been used as a means to increase receiver outlet temperatures to over 1000 $^{o}$C with inherent storage capabilities of the solid particles. Sand-like ceramic particles fall through a cavity receiver and are directly irradiated by concentrated sunlight. Once heated, the particles may be stored in an insulated tank and/or used to heat a secondary working fluid (e.g., steam, $CO_2$, air) for the power cycle. Because the solar energy is directly absorbed in the sand-like working fluid, the

flux limitations associated with tubular central receivers (high stresses resulting from the containment of high temperature, high pressure fluids) are avoided [71, 72]. As presented by Ho *et al*. [73], there are three main types of SPRs: B & W fluidized bed HX, Solex-shell-and-tube moving packed bed HX and VPE/solex-shell-and-plate moving packed bed HX. The directly irradiated SPR is a very useful design due to its ability to safely absorb high solar irradiance fluxes. The heat transfer fluid in the directly irradiated SPR should consist of solid particles that do not agglomerate or fracture, have a high solar weighted absorptivity and good chemical stability at high temperature. To this end, different numerical and experimental studies have been provided in this context [74-76]. Mathematical formula representing the efficiency of solid particle receivers, developed in the previous cited references, is given as follows:

$$\eta = \frac{Q_{part}}{Q_i} = \frac{\sum_{i=1}^{N} \dot{m}_i \, c_p \, (T_{i,f} - T_{i,o})}{Q_i} \qquad \text{(A1)}$$

where $\dot{m}_i$ is the mass flow rate of particle stream, $c_p$ is the particle specific heat, $T_{i,f}$ and $T_{i,o}$ are the final and initial particle temperatures, $Q_{part}$ is the power absorbed by the particles, and $Q_i$ is the total power entering the receiver.

### *3.2.2. Gas Receivers*

Volumetric Air Receivers

Volumetric air receivers have been under development since the 1980s [77]. In the volumetric air receiver, the concentrated solar radiation heats the material in the volume. At the same time, the working fluid passes through the volume and is heated up by forced convection, transforming the solar radiation into thermal energy.

The highly porous structure of volumetric receivers may be metal or ceramic. Since ceramics are the most appropriate materials for achieving the highest air temperatures, this is the most suitable option when temperatures above 800 $^{o}$C are necessary [**78**].

The two basic applications of volumetric air receivers are open-loop atmospheric receiver system for a Rankine cycle and closed-loop pressurized (windowed) receiver system for a Brayton Cycle [79, 80].

Small Particle Air Receivers

In small particle air receiver designs, submicron carbon particles are suspended in air and heated by concentrated sunlight in a pressurized cavity air-receiver. The energy is transferred to the pressurized air in the receiver for high-temperature Brayton cycles [81]. This heat-exchanger concept using solid–gas suspensions was first conceived in the1970s. Potential advantages include the following: solar radiation is absorbed throughout the gas volume due to the large cumulative surface area of the particles; higher incident fluxes with no solid absorber that can be damaged; particles are oxidized leaving a particle free outlet stream. Theoretical studies have shown that the receiver efficiency can reach up to 90 % depending on parameters such as particle size, particle concentration, optical properties of the particles and window, mass flow rate, and temperature [81-83]. Experiments conducted with a 25 $kW_{th}$ small-particle receiver showed that air could be heated to 700 $^{o}$C.

Tubular Gas Receivers

High-temperature solar thermal receivers have been proposed for air-Brayton cycles since the1970s, and prototypes have been developed and tested in recent years [84]. Early receiver designs were for parabolic dish receiver sand employed liquid-metal heat pipes to improve exchange heat from the solar irradiance to the gas. The internal heat-transfer coefficient in a liquid-metal heat pipe is on the order of 30,000 W/m$^2$ K compared to 300 W/m$^2$ K for heat transfer to gases. Therefore, higher solar fluxes can be tolerated with heat pipes yielding more compact receivers, lower metal temperatures, and lower pressure drops. Disadvantages include potentially higher receiver costs. Design specifications included an air-outlet temperature of 815 $^{o}$C with an air-inlet temperature of 565 $^{o}$C, air mass flow rate of 0.24 kg/s, pressure drop of 2%, and thermal efficiencies up to 85% [84-86].

### *3.2.3. Liquid Receivers*

Falling-Film Receivers

Falling-film receivers are characterized by gravity-driven fluid motion in the receiver. The fluid typically flows down an inclined wall and can either be directly irradiated or indirectly heated through the wall. This approach reduces the pumping requirement in the receiver.

***Direct-exposure falling-film receiver designs***: direct exposure falling-film receivers exploit absorption of the thermal energy directly by the receiver working fluid and reduce thermal resistance. Commonly, this approach has been referred to as a direct absorption receiver where the fluid is illuminated as it falls down an internal (cavity) or external wall. Blackened molten

nitrate salts (using suspended submicron particles) have been considered for these fluids so as to improve absorption in the liquid film. An optimum fluid layer opacity appears to exist for collection to maximize efficiency; optically thin layers of fluid do not adequately absorb direct illumination while opacities greater than the critical fluid layer thickness absorb near the surface resulting in greater emission. Addition of oxide dopants has been considered in molten salts to increase volumetric absorption in the transport fluid with reports of optical absorption properties with and without dopants reported in the literature [77, 87].

***Indirect-exposure falling-film receiver designs*:** to avoid the weaknesses of direct-absorption techniques and the exposure of the receiver working fluid to the environment, indirect-exposure internal film receiver designs have been proposed wherein the liquid film is on an internal surface of an inclined cavity wall **[88, 89]**. In this approach, the front side of the wall is heated by concentrated flux. However, the backside of this wall is in contact with the molten salt film. Therefore, the mechanism of heat transfer will be created when the fluid (salt film) flows and brings with it heat from the irradiated surface (front side). Numerous potential advantages of the internal film receiver as compared to salt-in-tube and direct absorption receivers have been outlined [77, 90].

Tubular Liquid Receivers

Tubular liquid central receiver systems have been studied since the 1970s and were first implemented in the1980s and 1990s in demonstration plants with Solar One and Solar Two [9, 91]. Conventional tubular receivers consist of an array of thin-walled tubes (stainless steel or alloyed) that are typically arranged to shuttle the working fluid (e.g., water/steam or molten salt) in multiple passes through incident concentrated sunlight [92]. The fluid is then transported to storage or to the power block. Two general receiver configurations occur: external and cavity. Prototypical designs for external and cavity receivers are illustrated in Figure **4**.

***Cavity tubular liquid receiver***: in a cavity receiver, the radiation reflected from the heliostats passes through an aperture into a box-like structure before impinging on the heat transfer surfaces; this box and aperture define the cavity. A receiver may be composed of more than one cavity, each facing a different sector of the heliostat field. However, recent studies of the cavity receiver concept indicate that the preferred configuration is a single cavity facing a north, in the northern hemisphere, heliostat field [93].

Tubular receiver designs are commonly comprised of several panels, which are in turn comprised of an array of tubes. Tubes in the same panel have fluid flows in the same direction and have approximately the same flux distribution. The use of numerous tubes effectively acts as a mechanism to enhance heat transfer, much like fins are used to increase surface area [77].

Other internal areas of the cavity, such as the roof and floor, do not normally serve as active heat absorbing surfaces. These areas must be effectively closed and insulated to minimize heat loss and to protect structure, headers, and interconnecting piping from incident flux. Although they are not exposed to high levels of direct flux, the inactive internal areas are exposed to radiation from the hot absorber panels. The inactive surfaces are typically uncooled and can reach temperatures exceeding those of the active panels. The active panel area and inactive internal surface area are each typically two to three times the area of the aperture. The aperture size and geometry are chosen to minimize the sum of thermal losses and spillage losses. A vertical aperture of square or rectangular shape is typical [93].

Temperatures of the heat transfer fluid exiting the receiver have been less than approximately 600 $^{o}$C to date. At elevated temperatures of 650 – 750 $^{o}$C, re-radiation effects must be considered in order to select an open or an enclosed receiver design. Liquid sodium and fluoride-salt heat-transfer fluids have also been proposed as an alternative to molten nitrate salt to achieve higher temperatures and efficiencies [77, 94].

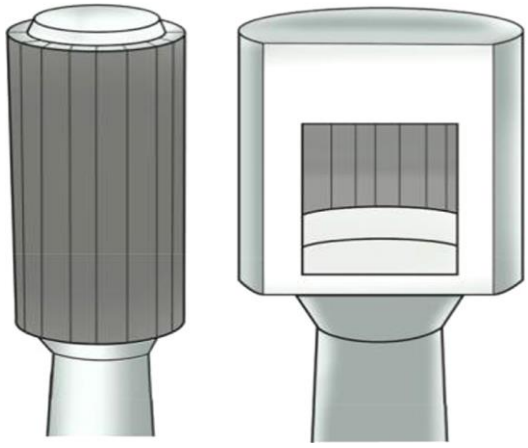

**Figure 4**: Schematics of tubular (left) external and (right) cavity receivers.

***External tubular liquid receiver***: external receivers have heat absorbing surfaces that are either flat, often

called a billboard, or convex toward the heliostat field [95]. For a large plant, an external receiver is typically a multipanel polyhedron that approximates a cylinder, with a surround heliostat field. The height to diameter ratio of a cylindrical receiver is generally in the range of 1 to 2. Smaller plants with external receivers typically use a north field configuration with a billboard or a partial cylinder receiver (omitting most of the south-facing panels) [63].

Estimated efficiencies for an external, tubular receiver employing a variety of working fluids (including high temperature HTFs such as LiCl/KCl and Na) indicate values in the 84–89% range appear achievable [16], with design point operation reaching above 90 % [16]. A final evaluation result of Solar Two's receiver indicates similar values and has become a standard for comparison. Additional fluids must also be considered (such as the fluorides) in order to achieve reasonable working fluid melting points and higher thermal conductivities that will improve efficiency. The fluid type is a limiting factor in the receiver operating temperature that, in turn, drives receiver efficiency [77, 96].

Major Components of Tubular Receiver

***Absorber panels***: absorber panels are fabricated in individual modules or subassemblies to facilitate handling during fabrication, shipment, and erection. It is desirable to have the modules designed to be completely interchangeable. Panel configuration for the molten salt receiver, illustrated in Figure **5**, is basically very similar to that of a conventional utility boiler panel. Each module consists of the panel tubes, inlet and outlet headers, buckstays, support struts, strongbacks, and insulation and sheathing (added during erection).

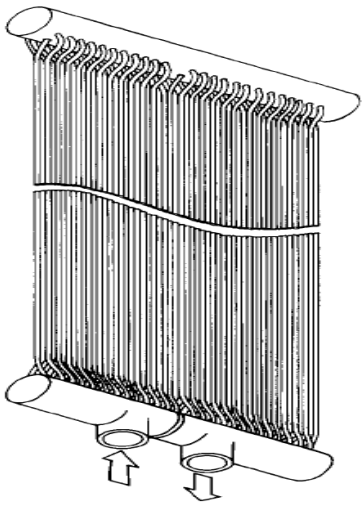

**Figure 5**: Typical receiver panel design [63].

***Receiver structure*****:** The main support structure for the receiver is required to carry the weight of the absorber panels, interconnecting piping and tanks, receiver heat transport fluid, and auxiliary items such as cranes or a cavity door. The structure must also withstand ice and wind loads and seismic effects. Seismic criteria provide the greatest uncertainty in the design and costing of the receiver structure. Standard structural steel columns, beams, and trusses are used.

***Heat transport media*****:** Four fluids have received most of the consideration for use as heat transport media. These fluids include water/steam, oil, molten salt, and liquid sodium. Salt, sodium, and water are the principal receiver fluid candidates. Oil has a lower operating temperature range and is generally envisioned only as a potential storage fluid in central receiver systems. Concerning the physical properties of these transport fluids we note that sodium has very high thermal conductivity while salt has a larger energy density. The viscosity of sodium is lower than salts.

Moreover, water/steam has a much lower freezing point than molten salt and liquid sodium and lacks some of the hazards associated with molten salt and liquid sodium. Water/steam is not a desirable storage medium; this configuration requires the exchange of thermal energy with a storage medium such as oil/rock. However, the use of oil as a heat transport fluid is limited to about 315 °C. The peak temperature limitation makes the oil unsuitable as a receiver medium for central receiver applications.

Molten salt is a relatively inexpensive and nontoxic heat transport and exchange fluid. Molten salt has been shown to be reliable and safe as a heat transport medium when proper design considerations and adequate precautions are taken. Molten salt is a desirable medium as a receiver and storage fluid because it is stable up to temperatures of about 595°C and remains liquid down to temperatures near 245 °C.

Sodium has excellent heat transfer properties allowing high-flux small receivers. It is, however, a more expensive, less dense medium and has a lower specific heat than molten salt. In general, the operation of liquid sodium systems is similar to molten salt systems. One major difference is the reactivity of sodium when in contact with air or water.

***Instrumentation and controls*****:** The receiver control system has two primary functions: to maintain the receiver heat transport fluid outlet conditions at set

point values during normal operations, and to operate and protect the receiver during transient and emergency conditions such as start-up, shutdown, cloud passages, and equipment/component failure. Because of input power and flux distribution changes caused by diurnal and meteorological conditions, the control system must vary the receiver heat transport fluid flow rate to maintain outlet temperature and pressure at the desired set point. Sensors used in the receiver control system may include thermocouples, pressure transducers, flux transducers, flow meters, and fluid level indicators. Control systems typically operate on feedback output from sensors that measure receiver outlet conditions. However, the use of feed-forward data (particularly flux levels) may be helpful.

Receiver control is closely tied to heliostat field control during start-up and shutdown. Once the full heliostat field is focused on the receiver, control of receiver outlet conditions to accommodate varying levels of insolation is achieved primarily by adjustments to the receiver feed pump flow rate, and secondarily by adjustments to valves controlling parallel flow paths in the receiver. In a once-through receiver each panel requires a flow control valve, while for a multipass receiver each control zone requires its own control valve [16].

***Absorber surface design*:** The active receiver absorber surface area is an important factor affecting receiver cost and receiver performance. With the exception of spillage losses, all other cost and performance criteria favor minimizing the active area. However, structural integrity requirements limit the maximum flux that a receiver absorber surface can withstand for a given lifetime [97, 98].

## 4. MODELING OF SOLAR TOWER POWER PLANTS

In general, three different methods are used by the researchers for the modeling of STPP performances and reliability: the analytical method, the numerical method and the artificial intelligence method (AI). To date, many groups of scholars have done much important work concerning the modeling and simulation of STPP using these different methods. The first group mainly focuses on the thermal losses analysis of the solar cavity receiver and many analytical models for the estimation of thermal losses were proposed [99-104]. Furthermore, many other scholars have also worked on the thermal losses calculation which are listed in [31, 105-108]. The second group of research within the modeling of the STPP was mainly focused on the modular modeling of the whole system. In these studies, the main objective was to calculate the power output of the STPP using the energy balance [21-24, 26-28, 31, 32, 109]. The third group concentrated on the use of various numerical methods and models in order to assess the reliability of the different components of STPP [39, 43, 66]. All these groups used traditional regressive models that can be solved either numerically or analytically. Some of the drawbacks are that they use a large number of parameters, empirical correlations for heat transfer and sometimes there is the possibility of no convergence [110]. To address this problematic, another research group turned to the use of the artificial intelligence (AI) techniques, such as artificial neural network method (ANN). This later (ANN) offers an alternative way to tackle complex and ill-defined problems [111]. ANN method has been used by several authors in the field of solar energy; for modeling and design of a solar steam generating plant, for the estimation of a parabolic-trough collector's intercept factor and local concentration ratio and for the modeling and performance prediction of solar water-heating systems [19, 112-114], for prediction of solar irradiance [115, 116], for the modeling of the solar collectors [19, 117] and for the modeling of STPP receiver [118].

### 4.1. Modeling of the Heliostat

Heliostats are the most important cost element of a solar power tower plant [26]. Since they constitute about 50% to the capital cost of the plant, it is important to reduce the cost of heliostats to as low as possible to improve the economic viability of power towers [119]. Therefore, reliable, performant and optimized heliostat design are the important factors to minimize this cost. To address this problematic, several research works have been done on heliostat systems. This research can be grouped into four main groups.

The first group mainly focuses on the heliostat field layout optimization, such as [21, 22, 119-127]. The second group has investigated the wind load effect on heliostats [128, 132-135]. The third group of researchers has worked on the design and optical performance of the heliostat [136, 137]. Zang *et al*. [136] have optimized the heliostat structure in order to reduce the manufacturing cost. The last group discusses the heliostat reliability analysis [43, 44, 138, 139].

### 4.2. Modeling of the Receiver

Main thermodynamic formula and laws used for the energy analysis of the STPP are the conservation

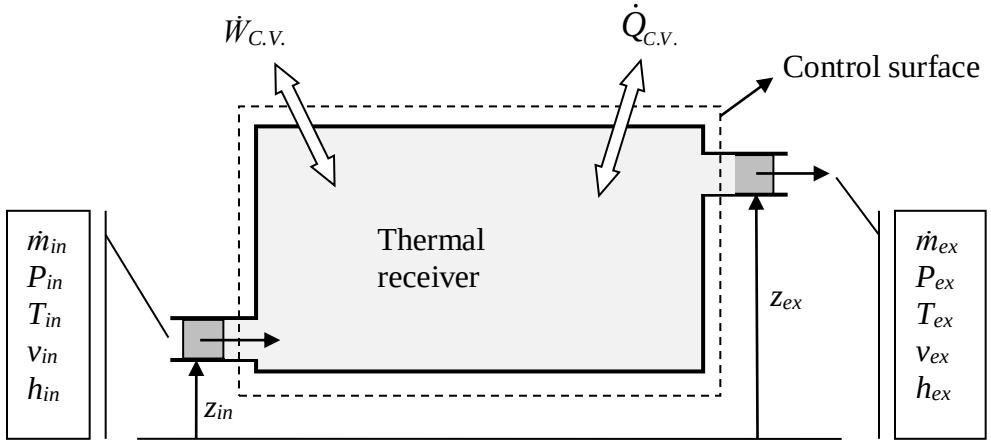


**Figure 6:** Control volume for energy balance analysis.

equation of mass, the first law of thermodynamics and the equations of state [140]. The first law of Thermodynamics deals with conservation of energy in a process. In order to establish the, energy conservation equation we consider the schematics in Figure **6**.

The first law of thermodynamics for a control volume can be expressed as Eq. **(A2)**:

$$\left(\frac{dE}{dt}\right)_{C.V.} = \sum_{\text{in}} \dot{m}_{in}\left(h_{in} + \overline{KE_{in}} + \overline{PE_{in}}\right) - \sum_{ex} \dot{m}_{ex}\left(h_{ex} + \overline{KE_{ex}} + \overline{PE_{ex}}\right) + \sum_{\text{j}} \dot{Q}_{\text{j}} - \dot{W}_{C.V.} \quad \text{(A2)}$$

*E* is the total energy which is the instantaneous total energy within the control volume.

*h* is the specific enthalpy which is the sum of the specific internal energy and the product of pressure *P* versus specific volume, *v*. The SI unit is kJ/kg.

$\overline{KE}$ is the specific kinetic energy (energy per unit mass), is written as:

$\overline{KE} = V^2/2$ , V is the velocity.

$\overline{PE}$ is the specific gravitational potential energy which is the multiplication of the acceleration of gravity *g* and the elevation *z*.

$\overline{PE} = gz$

The subscripts *in* and *ex* stand, respectively, for the inlet and the outlet of the system.

$\dot{W}$ is the shaft power which is the mechanical power produced or absorbed by the rotating shaft of the thermal machine.

$\dot{Q}$ is the thermal power which is the form of energy rate transferred to or from the machine due to a difference of temperatures between the machine and the surroundings, the higher temperature to the lower one.

The effect of the incident heat flux on the receiver efficiency is reported in Figure **7**. For small STPP capacities (under 2 MW) this efficiency is approved by the majority of authors [26].

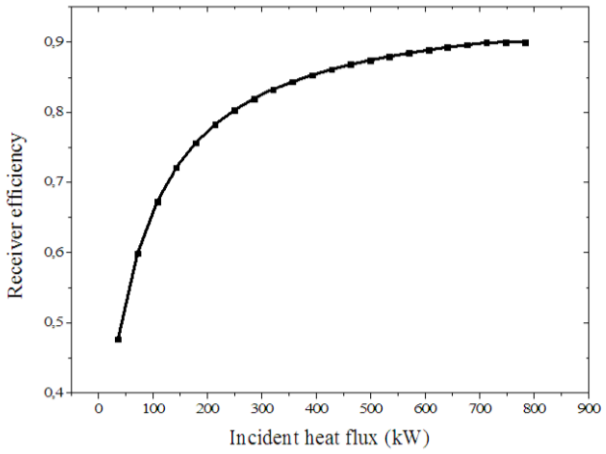


**Figure 7**: Effect of the incident heat flux on the receiver efficiency [26].

### 4.3. Modeling of the Power Cycle Subsystem

The power cycle subsystem is, generally, represented by Ranking, Brayton or combined cycle (Ranking and Brayton). The STPP with combined cycle, as

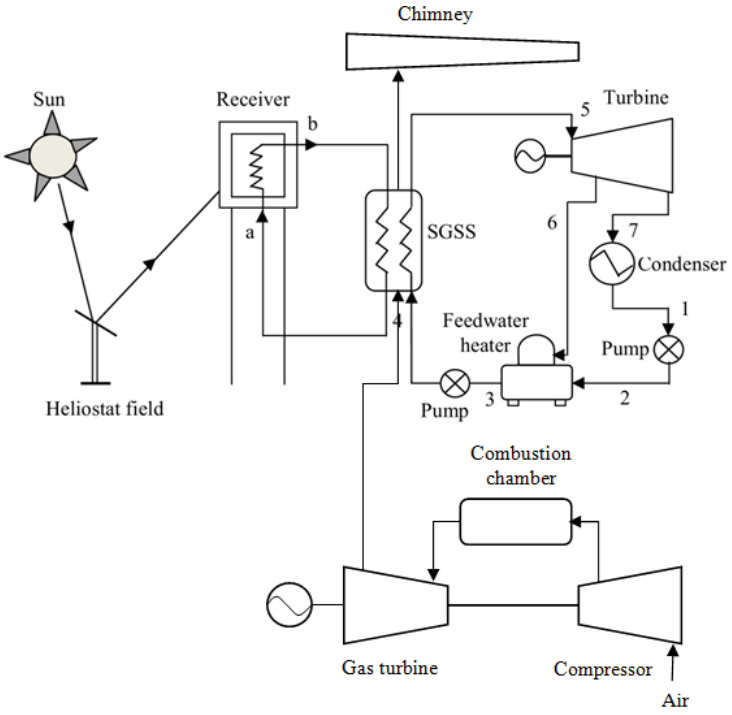


**Figure 8**: Schematic of a hybrid solar-gas tower power plant.

shown in Figure **8**, is called: hybrid solar-gas tower power plant (HSTPP).

The efficiency of HSTPP is given by [62]:

$$\eta_{HSTPP} = \frac{\dot{W}_B + \eta_{STPP} \times (\dot{Q}_B - \dot{W}_B)}{\dot{Q}_B} = \eta_B + \eta_{STPP} - \eta_B \times \eta_{STPP} \quad \text{(A3)}$$

where,

$\dot{W}_B$ is the power generated by the Brayton cycle, $\dot{Q}_B$ is the heat lost by the Brayton cycle, $\eta_{STPP}$ is the STPP efficiency and $\eta_B$ is the Brayton cycle efficiency.

In Figure **9**, the effect of the STPP efficiency on the HSTPP efficiency has been illustrated. In this figure it can be seen that the HSTPP efficiency increases with the increasing of the STPP efficiency. In literature, this result has been validated by several authors [**62**].

The various works published on the modeling of different components of STPP have summarized in Table **3**. The modeling method, the obtained results and the limitations of the used method are also presented in this table.

## 5. CONCLUSION

In this review, brief description and comparison, including fundamentals, of the different CSP technologies are provided. Though most of the installed CSP is of parabolic trough technology, the central receiver system (solar tower) technology is gaining ground and is under consideration worldwide for many projects.

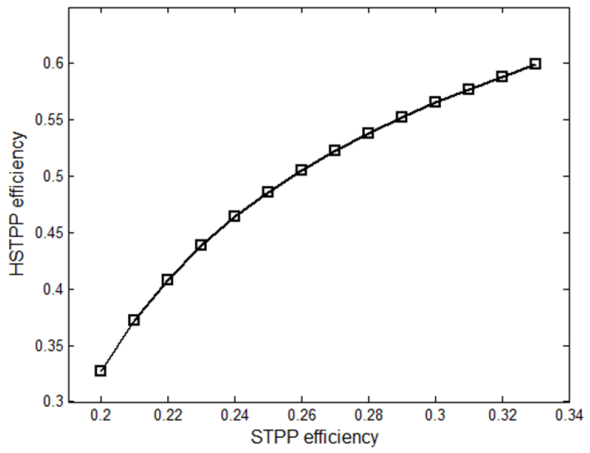


**Figure 9**: Effect of the STPP efficiency on the HSTPP efficiency [62].

In addition, a detailed description of the different types of solar power plants with central receiver system (solar tower power plants) is presented. It is concluded that about half of the research studies have been focused on solar receiver. On this topic, a high percentage of these studies has dealt with cavity and external receivers, while a lower percentage with volumetric receivers and we have found that there has

**Table 3: Summary of the Various Works Published on the Modeling of STPP**

| Component | References | Method of Modeling | Results | Limitations |
|---|---|---|---|---|
| Whole system | [27] | Analytical | Calculation of STPP output power using energy balance | - |
| | [28] | Analytical | Development of dynamic models for use in simulation and control of STPP | - |
| | [31] | Analytical | The design of a global steady-state thermal model of a 100 kWt STPP was developed | The developed model is only applicable for the steady state |
| | [141] | Analytical and numerical | The authors have simulated models of performance, reliability, and cost taking into consideration the uncertainties in the performance model of a typical STPP example. | The method used in this study (Latin hypercube sampling) is less accurate with small probabilities. |
| | [22] | Analytical | In this study, the authors have given a theoretical framework for the energy and exergy analysis of the STPP using molten salt as the heat transfer fluid. Therefore, both the energy losses and exergy losses in each component and in the overall system are evaluated to identify the causes and locations of the thermodynamic imperfection. | The authors have not taken into account all the parameters such as the mass flow of the HTF in each tube. |
| | [23] | Analytical | 1 MW Dahan solar thermal power tower plant is modeled from mathematical models for all of the working conditions using the modular modeling method. | Modular modeling method needs a lot of calculation |
| | [24, 32] | Analytical and numerical | The authors have Simulated and analyzed the performances of central cavity receiver of STPP. They have found that the wind conditions can obviously affect the thermal losses and the value reaches its maximum when the wind blows from the side of the receiver. | - |
| | [26] | Analytical | The have developed a mathematical model in order to simulate the performances of STPP without storage. The developed model is accurate to simulate all thermal and thermodynamic parameters in STPP. | The authors have not taken into account the storage system |
| | [62] | Analytical, Numerical and AI | The author has given a general and a deep study of the dependability of STPP using three different methods. | - |
| Receiver | [99, 100] | Analytical | Thermal losses analysis of the solar cavity receiver | The resolution of the developed model needs an efficient numerical method |
| | [101] | Numerical | The authors have presented a numerical method, based on finite differences, for the study of combined natural convection and radiation in a rectangular, two-dimensional cavity containing a non-participating (i.e. transparent) fluid. | The authors have not taken into account the heat losses through all the walls of receiver. |
| | [102] | Numerical and experimental | Experimental investigation of natural convection heat loss from a model solar concentrator cavity receiver | - |
| | [103] | Analytical | The authors have Investigated the approximate estimation of the natural convection heat loss from an actual geometry of the modified cavity receiver | - |
| | [104] | Analytical | The authors have presented an experimental and numerical study of the steady state convective losses occurring from a downward facing cylindrical cavity receiver of length 0.5 m, internal diameter of 0.3 m and a wind skirt diameter of 0.5 m.<br>It is found that the convective loss increases with mean receiver temperature and decreases with increase in receiver inclination. Nusselt number correlations are proposed for two receiver fluid inlet temperature ranges, 50 –75 °C and 100 – 300 °C, | - |
| | [39, 118] | AI | The authors have analyzed the reliability and performances of STPP using artificial neural network method (ANN). This method has presented a good accuracy with the analytical results. | - |

**(Table 3) contd….**

| Component | References | Method of Modeling | Results | Limitations |
|---|---|---|---|---|
| Collector | [19] | AI | The published document has given an overview on the different AI methods used for the optimization and modeling of solar collectors. | - |
| | [115] | AI | The authors have estimated thermal performances of solar air collectors using artificial neural network method (ANN). The calculated values of thermal performances are compared to predicted values. Therefore, the comparison demonstrates the effectiveness of the proposed ANN. | - |
| | [120] | Numerical | The published paper deals with the optimization of heliostat field layout.<br>It was found from the plotted results that the minimum radial spacing is a function of the distance from the tower measured in tower height, the location of the site, the operation time of the plant, and to some extent the position angle of the heliostats. | The method should be applied for more number of units and for large heliostat field |
| | [121] | Analytical | Mathematical formulation of a graphical method for a no-blocking heliostat field layout. | - |
| | [122] | Numerical | Methodology for generation of heliostat field layout in central receiver systems based on yearly normalized energy surfaces. | - |
| | [136] | Numerical | The authors have developed a multi-objective thermo-economic optimization for the design of heliostat field of STPP.<br>Two objectives (specific energy cost versus investment cost) have been taken into account. | The method is limited to two objectives only. |
| | [21] | Numerical | A software tool HFLD is developed for heliostat field layout design and performance calculation. The simulation results from HFLD approximately agree very well with the published heliostat field efficiency data from Spain PS10 | - |
| | [124] | Numerical | Development of an algorithm for optimizing the field layout, based on the performance function that includes heliostat characteristics, secondary optics, and chemical receiver–reactor characteristics at representative time steps for evaluating the annual fuel production rates. | - |
| | [125] | Numerical | The authors developed a code to generate a regular heliostat field, called campo.<br>The code *campo*, based on the Matlab type cell data structure, is able to generate regular but flexible radial staggered layouts of heliostat fields. | - |
| | [126] | Numerical | The authors have developed a model and a biomimetic pattern for heliostat field layout optimization.<br>The model, described and validated herein, includes a detailed calculation of the annual average optical efficiency accounting for cosine losses, shading and blocking, aberration and atmospheric attenuation. | - |
| | [127] | Numerical | Continuous heliostat field optimization is studied by the authors as an alternative to patterns. They have designed a general method (Hector) to support continuous field optimization. | - |
| Heliostat unit | [64] | Analytical | The part-load behavior of a typical 30-MWe SEGS (solar electric generating systems) plant was studied using a detailed thermodynamic model.<br>The model was also compared to the SOLERGY model, showing differences between the assumptions used in both models | the model still lacks the capability to fully account for actual solar field conditions. |
| | [128] | Experimental and analytical | The author has investigated the wind load effect on heliostats. A comparison of data obtained from wind tunnel tests with analytical results is presented. Testing consisted of obtaining loads, moments, dynamic behavior (via servo accelerometers) and flow visualization for the entire range of operational and survival configurations. | - |

**(Table 3) contd….**

| Component | References | Method of Modeling | Results | Limitations |
|---|---|---|---|---|
| | [129, 130] | Experimental and analytical | The authors have developed a design method to define wind loads on flat heliostat. The tests investigated primarily the mean forces, moments, and the possibility of measuring fluctuating forces in anticipation of reducing those forces. | The effects of porosity in the collectors is not addressed. |
| | [119] | Experimental and analytical | It can be demonstrated from this study that the design-relevant wind load coefficients are not Reynolds number dependent. However, the inclination of the mirror plane in stow position, due to the deflection of the heliostat's structure at high Reynolds number, leads to increased wind loads. | - |
| | [132] | Numerical | A finite element model is developed to calculate the wind-induced displacement, the equivalent stress and the structural natural vibration frequency of the heliostat. The results show that, under fluctuating wind pressure, the maximum displacement of the structure occurred at corners of upper parts and the level of the maximum equivalent stress in the rotation axis is higher than that in other components of the heliostat. | Long computing time |
| | [133] | Numerical | The authors have proposed a numerical simulation method for wind loads fluctuations on heliostats and they have analyzed the dynamic response of the heliostat.<br>For the simulated acceleration, the dominant frequency value of 3.16 Hz had the highest probability of occurrence compared with 3.18 Hz tested acceleration. | Methods for wind-load simulation or calculation should be explored to further improve the simulation accuracy. |
| | [134] | Experimental and numerical | An experimental and numerical modal analysis was performed on an 8 $m^2$ T-shaped heliostat structure at different elevation angles.<br>The agreement between experiments and simulations is good in all operating points investigated | - |
| | [135] | Numerical | An ANSYS Fluent CFD model of a single heliostat in some worst-case positions is produced using numerical simulations with the realizable k-ε model.<br>It is shown that the coefficients are sensitive to the clearance gap. More specifically, there is a compromise between lift and drag, and a specific HCL is beneficial to minimize the hinge moment. | Long computing time |
| | [137] | Numerical | Design, optimization and optical performance study of tripod heliostat for solar power tower plant | This type of heliostat still not realizable for large mirrors |
| | [138] | Experimental and analytical | Demonstration of the role of structural dynamic tests (also known as modal tests) to provide a characterization of the important dynamics of the heliostat structure as they relate to durability and optical accuracy.<br>The use of structural dynamic tests to provide data to evaluate and improve the accuracy of computer-based design models.<br>The selection of sensors and data-processing techniques that are appropriate for long-term monitoring of heliostat motions. | - |
| | [139] | Analytical | The author has analyzed the importance of various effects on heliostat drive unit life, including wind conditions, angles of attack, size, and endurance limits and how these affect predicted safety factors required in terms of fatigue damage | - |
| | [43, 44] | Analytical | The authors have developed a structural reliability model for heliostat unit in order to assess, under stochastic wind load, the reliability level of a given heliostat system design. | - |

been a little interest in the particle receivers. To this end, the main components of cavity and external receivers are described.

Based on an extensive bibliographical research, it can be concluded that there are two main methods to model and simulate the performances and reliability of

STPP: the analytical method and artificial neural network method (ANN). It has been found that the most research studies focused on the analytical approach. On the other hand, fewer scholars used the ANN method for the modeling and simulation of STPP.

## NOMENCLATURE

$c_p$ : specific heat, J/kg K.

$\overline{KE}$ : specific kinetic energy, J/kg.

$\dot{m}_i$ : the mass flow rate, kg/s.

$\dot{Q}_B$ : heat lost by the Brayton cycle, Watt.

$Q_i$ : power entering the receiver, Watt.

$Q_{part}$: power absorbed by the particles, Watt.

$\overline{PE}$ : specific gravitational potential energy, J/kg.

$T_{i,f}$: final particle temperature, K.

$T_{i,o}$ : initial particle temperature, K.

*V:* velocity, m/s.

*Ẇ*: shaft power, Watt.

$\dot{W}_B$ : power generated by the Brayton cycle, Watt.

$\eta_{STPP}$ : STPP efficiency and,

$\eta_B$ : Brayton cycle efficiency,

## ABBREVIATIONS

| | | |
|---|---|---|
| ANN | = | Artificial neural network |
| AI | = | Artificial intelligence |
| CFD | = | computational fluid dynamics |
| CSP | = | Concentrating solar power technologies |
| HSTPP | = | Hybrid solar-gas tower power plant |
| HTF | = | Heat transfer fluid |
| O&M | = | Operations and maintenance |
| PV | = | Photovoltaics |
| SPRs | = | Solid particle receivers |
| SRC | = | Short rotation coppice |
| STPP | = | Solar tower power plant |

## REFERENCES


[1] Sözen Adnan, Menlik Tayfun, Ünvar Sinan. Determination of efficiency of flat-plate solar collectors using neural network approach. Expert Systems with Applications 35 (2008) 1533-1539.
https://doi.org/10.1016/j.eswa.2007.08.080

[2] Zhang M, Mu HL, Ning YD. "Accounting for energy related CO2 emission in China, 1991-2006". Energy Policy 2009; 37:767-73.
https://doi.org/10.1016/j.enpol.2008.11.025

[3] Chen G.Q., Yang Q., Zhao Y.H., Wang Z.F. "Nonrenewable energy cost and greenhouse gas emissions of a 1.5 MW solar power tower plant in China", Renewable and Sustainable Energy Reviews 15 (2011) 1961-1967.
https://doi.org/10.1016/j.rser.2010.12.014

[4] Imadojemu H. E., "concentrating parabolic collectors: a patent survey", Energy Conversion and Management Vol.36, No. 4, pp. 225-237, 1995.
https://doi.org/10.1016/0196-8904(94)00058-8

[5] Hennecke, K; Dersch, J & Quaschning, V. Greenius - a simulation tool for renewable energy utilization. In: SolarPACES 2010 Conference, Perpignan, France (2010).

[6] Pedraza J. M. Solar Energy in Cuba: Current Situation and Future Development. Journal of Solar Energy Research Updates, 2019, 6, 1-14.

[7] Pedraza J. M. Solar Energy in Latin America and the Caribbean: The Current Situation and Perspectives in the Use of Solar Energy for Electricity Generation. Journal of Solar Energy Research Updates, 2020, 7, 17-41.

[8] Şen Z. Solar energy fundamentals and modeling techniques: atmosphere, environment, climate change and renewable energy. 2008 Springer-Verlag London Limited.

[9] Kalogirou SA. Solar Energy Engineering: Processes and Systems. 2nd edition, ISBN: 0123972701. Elsevier Inc, USA, 2014.

[10] Twidell J, Weir T, Renewable energy resources, Taylor & Francis, London and New York, 2006.
https://doi.org/10.4324/9780203478721

[11] Boudries R. Analysis of solar hydrogen production in Algeria: Case of an electrolyzer-concentrating photovoltaic system, International journal of hydrogen energy 38 (2013) 11507 - 11518.
https://doi.org/10.1016/j.ijhydene.2013.04.136

[12] Desideri Umberto, Elia Campana Pietro. Analysis and comparison between a concentrating solar and a photovoltaic power plant. Applied Energy 113 (2014) 422-433.
https://doi.org/10.1016/j.apenergy.2013.07.046

[13] Soulayman S. and Hababa M. A. The Solar Panel's Performance Dependence on Incident Radiation Intensity and its Surface Temperature. Journal of Solar Energy Research Updates, 2017, 4, 9-17.
https://doi.org/10.15377/2410-2199.2017.04.2

[14] Plourde B.D., Gikling A., Marsh T., Riemenschneider M.A., Fitzgerald J.L., Minkowycz W.J., Kiplagat J. and Abraham J.P. Design and Evaluation of a Concentrated Solar-Powered Thermal-Pasteurization System. Journal of Solar Energy Research Updates, 2019, 6, 34-42.

[15] Barlev D, Vidu R, Stroeve P. Innovation in concentrated solar power. Solar Energy Materials & Solar Cells 95(10): (2011) 2703-25.
https://doi.org/10.1016/j.solmat.2011.05.020

[16] Rosen MA, Dincer I., "Exergy-cost-energy-mass analysis of thermal systems and processes". Energy Conversion and Management 2003; 4(10):1633-51.
https://doi.org/10.1016/S0196-8904(02)00179-6

[17] Mondol J. D. and Jacob G. Commercial Scale Solar Power Generation (5MW to 50 MW) and its Connection to Distribution Power Network in the United Kingdom. Journal of Solar Energy Research Updates, 2018, 5, 25-38.

[18] Patel Mukund R., "Wind and Solar Power Systems" Merchant Marine Academy Kings Point, New York; CRC Press 1999.

[19] Kalogirou SA. Solar thermal collectors and applications, Progress in Energy and Combustion Science 30 (2004) 231-295.
https://doi.org/10.1016/j.pecs.2004.02.001

[20] Tyagi SK, Wang Shengwei, Singhal MK, Kaushik SC, Park SR. Exergy analysis and parametric study of concentrating type solar collectors. International Journal of Thermal Sciences 46 (2007) 1304-1310.
https://doi.org/10.1016/j.ijthermalsci.2006.11.010

[21] Yao Z, Wang Z, Lu Z, Wei X. "Modeling and simulation of the pioneer 1MW solar thermal central receiver system in China", Renewable Energy 34 (2009) 2437-2446.
https://doi.org/10.1016/j.renene.2009.02.022

[22] Xu C, Wang Z, Li X, Sun F. Energy and exergy analysis of solar power tower plants. Applied Thermal Engineering, 2011, 31, 3904-3913.
https://doi.org/10.1016/j.applthermaleng.2011.07.038

[23] Xu E, Yu Q, Wang Z, Yang C. Modeling and simulation of 1 MW DAHAN solar thermal power tower plant. Renewable Energy, 2011, 36, 848-857.
https://doi.org/10.1016/j.renene.2010.08.010

[24] Yu Q, Wang Z, Xu E. "Simulation and analysis of the central cavity receiver's performance of solar thermal power tower plant", Solar Energy 86 (2012a) 164-174.
https://doi.org/10.1016/j.solener.2011.09.022

[25] McGovern Ronan K., Smith William J., "Optimal concentration and temperatures of solar thermal power plants", Energy Conversion and Management 60 (2012) 226-232.
https://doi.org/10.1016/j.enconman.2011.11.032

[26] Benammar S, Khellaf A, Mohammedi K. Contribution to the modeling and simulation of solar power tower plants using energy analysis. Energy Conversion and Management, 2014a, 78, 923-930.
https://doi.org/10.1016/j.enconman.2013.08.066

[27] Ferriere A, Bonduelle B, Amouroux M. Development of an optimal control strategy for the thémis solar plant: Part 1 - Themis transient model. Transactions of the ASME 111, (1989) 298-304.
https://doi.org/10.1115/1.3268326

[28] Yebra LJ, Berenguel M, Dormido S, Romero M. "Modeling and simulation of central receiver solar thermal power plants", In: Proceedings of the 44th IEEE Conference (2005), Spain.

[29] Buck Reiner, Barth Christian, Eck Markus, Steinmann Wolf-Dieter. Dual receiver concept for solar towers. Solar Energy 2006;80: 1249-54.
https://doi.org/10.1016/j.solener.2005.03.014

[30] Wei Xiudong, Lu Zhenwu, Wang Zhifeng, Yu Weixing, Zhang Hongxing, Yao Zhihao. A new method for the design of the heliostat field layout for solar tower power plant. Renewable Energy 2010; 35: 1970-1975.
https://doi.org/10.1016/j.renene.2010.01.026

[31] Li, X; Kong, W; Wang, Z; Chang, C & Bai, F. Thermal model and thermodynamic performance of molten salt cavity receiver. Renewable Energy, 2010, 35, 981-988.
https://doi.org/10.1016/j.renene.2009.11.017

[32] Yu Q, Wang Z, Xu E, Li X. Minghuan Guo, "Modeling and dynamic simulation of the collector and receiver system of 1MWe DAHAN solar thermal power tower plant", Renewable Energy 43 (2012b) 18-29.
https://doi.org/10.1016/j.renene.2011.11.040

[33] Ben-Zvi R, Epstein M, Segal A. Simulation of an integrated steam generator for solar tower. Solar Energy 2012; 86: 578-592.
https://doi.org/10.1016/j.solener.2011.11.001

[34] Montes, MJ; Abánades, A & Martínez-Val, JM. Performance of a direct steam generation solar thermal power plant for electricity production as a function of the solar multiple. Solar Energy, 2009, 83, 679-689.
https://doi.org/10.1016/j.solener.2008.10.015

[35] Sahoo Sudhansu S, Singh Suneet, Banerjee Rangan. Analysis of heat losses from a trapezoidal cavity used for Linear Fresnel Reflector system. Solar Energy 2012; 86: 1313-1322.
https://doi.org/10.1016/j.solener.2012.01.023

[36] Matteson T D and Smith A M. Application of reliability-centered maintenance to solar central receiver plants. United States: N. p., 1986. Web. doi:10.2172/5258788.
https://doi.org/10.2172/5258788

[37] Kolb G J. Reliability Analysis of a Salt-in-Tube Central Receiver Power Plant. Sandia National Laboratories report Albuquerque (1990), NM, pp. 19.

[38] Fork, D.K., Fitch, J., Ziaei, S., Jetter, R.I., 2012. Life estimation of pressurized-air solar-thermal receiver tubes. J. Solar Energy Eng. 134 (4), 041016.
https://doi.org/10.1115/1.4007686

[39] Benammar S, Khellaf A, Mohammedi K. Solar tower power plants performance and reliability analysis. In: solar power, Editor: Stephen Bailey. Nova science publishers, Inc. ISBN: 978-1-63321-317-3. USA, 2014b.

[40] Setien E., Frasquet M., G. Saliou, M. Silva, G. Pinna, R. Blázquez, V. Ruiz. Reliability analysis of Solar-Gas Hybrid Receivers for central tower plants. Energy Procedia 69 (2015) 1558 - 1567.
https://doi.org/10.1016/j.egypro.2015.03.108

[41] Conroy T., Collins M. N., Fisher J., Grimes R., (2018). Levelized cost of electricity evaluation of liquid sodium receiver designs through a thermal performance, mechanical reliability, and pressure drop analysis. Solar Energy 166, 472-485.
https://doi.org/10.1016/j.solener.2018.03.003

[42] Benammar S and Khellaf A. Solar Tower Power Plant Reliability Analysis using FORM method. 3ème Conférence Internationale de Mécanique (ICM' 2017), Annaba 26-27 Avril 2017.

[43] Benammar S., Tee K F. Structural reliability analysis of a heliostat under wind load for concentrating solar power. Solar Energy 181 (2019) 43-52.
https://doi.org/10.1016/j.solener.2019.01.085

[44] Benammar S, Tee K F. Failure probability analysis of heliostat systems. Int. J. Critical Infrastructures, Vol. 16, No. 4, 2020.
https://doi.org/10.1504/IJCIS.2020.112037

[45] Romero-Alvarez Manuel, Zarza Eduardo. Concentrating solar thermal power. 2007 by Taylor & Francis Group, LLC.

[46] Ummadisingu A, Soni MS, Concentrating solar power - technology, potential and policy in India. Renewable and Sustainable Energy Reviews 15(9): (2011) 5169-75.
https://doi.org/10.1016/j.rser.2011.07.040

[47] Alexopoulos S., Hoffschmidt Bernhard, "Solar tower power plant in Germany and future perspectives of the development of the technology in Greece and Cyprus", Renewable Energy 35 (2010) 1352-1356.
https://doi.org/10.1016/j.renene.2009.11.003

[48] Pavlović Tomislav M., Radonjić Ivana S., Milosavljević Dragana D., Lana S. Pantić. A review of concentrating solar power plants in the world and their potential use in Serbia. Renewable and Sustainable Energy Reviews 16 (2012) 3891- 3902.
https://doi.org/10.1016/j.rser.2012.03.042

[49] Zhang HL, Baeyens J, Degrève J, Cacères G. Concentrated solar power plants: Review and design methodology. Renewable and Sustainable Energy Reviews 22 (2013) 466-481.
https://doi.org/10.1016/j.rser.2013.01.032

[50] Blair N, Mehos M, Christensen C. Sensitivity of concentrating solar power trough performance, cost and financing with the Solar Advisor Model. NREL CD-550-42702, pp. 1-8 (2008).

[51] Cavallaro F. Multi-criteria decision aid to assess concentrated solar thermal technologies. Renewable Energy 34(7): (2009) 1678-85.
https://doi.org/10.1016/j.renene.2008.12.034

[52] Janjai S., Laksanaboonsong J., Seesaard T., Potential application of concentrating solar power systems for the generation of electricity in Thailand. Applied Energy 88 (2011) 4960-4967.
https://doi.org/10.1016/j.apenergy.2011.06.044

[53] Becker M, Klimas PC. Second-Generation Central Receiver Technologies: A Status Report, eds. Muller CF, Karlsruhe, Germany (1993).

[54] Braun FG, Hooper E, Wand R, Zloczysti P. Holding a candle to innovation in concentrating solar power technologies: a study drawing on patent data. Energy Policy 39(5): (2011) 2441-56.
https://doi.org/10.1016/j.enpol.2011.02.008

[55] Patel Mukund R. Wind and solar power systems: design, analysis, and operation. CRC Press Taylor & Francis Group, 2006.
https://doi.org/10.1201/9781420039924

[56] Sharma A. A comprehensive study of solar power in India and World. Renewable and Sustainable Energy Reviews 15(4): (2011) 1767-76.
https://doi.org/10.1016/j.rser.2010.12.017

[57] Zhu Guangdong, Wendelin Tim, Wagner Michael J., Kutscher Chuck. History, current state, and future of linear Fresnel concentrating solar collectors. Solar Energy, 103 (2014) 639-652.
https://doi.org/10.1016/j.solener.2013.05.021

[58] Răboacă M. S., Badea G., Enache A., Filote C., Răsoi G., Rata M., Lavric A. and Felseghi R-A. Concentrating Solar Power Technologies. Energies 2019, 12, 1048.
https://doi.org/10.3390/en12061048

[59] Droher J.J., Squier S.E. Performance of the Vanguard Solar Dish-Stirling Engine Module, EPRI AP-4608, Electrical Power Research Institute, Palo Alto, CA (1986).

[60] Hijazi H., Mokhiamar O., Elsamni O. Mechanical design of a low cost parabolic solar dish concentrator. Alexandria Engineering Journal. Vol 55, Issue 1, March 2016, Pages 1-11.
https://doi.org/10.1016/j.aej.2016.01.028

[61] Smith DC, Chavez JM. A final report on the phase I testing of a molten-salt cavity receiver, Sandia National Laboratories, SAND 87-2290.

[62] Benammar S., (2015), Contribution to the Dependability of Hybrid Solar / Gas Tower Power Plants. PHD thesis, University M'Hemd Bougara-Boumerdes.

[63] Falcone PK. A Handbook for Solar Central Receiver Design, Sandia National Laboratories, Livermore, CA. December, 1986. Report SAND 86-8009.
https://doi.org/10.2172/6545992

[64] Reddy R G. Novel Molten Salts Thermal Energy Storage for Concentrating Solar Power Generation. Final Scientific/Technical Report. October 2013, United States Department of Energy.
https://doi.org/10.2172/1111584

[65] Fernandez A. G., Galleguillos H., Fuentealba E., Perez F. J. Thermal characterization of HITEC molten salt for energy storage in solar linear concentrated technology. J Therm Anal Calorim (2015) 122:3-9. DOI 10.1007/s10973-015-4715-9.
https://doi.org/10.1007/s10973-015-4715-9

[66] Lippke, F. Simulation of the Part-Load Behavior of a 30 MWe SEGS Plant, SANDIA Report SAND95-1293 (1995).
https://doi.org/10.2172/95571

[67] Smith DC, Chavez JM. A final report on the phase I testing of a molten-salt cavity receiver, Sandia National Laboratories, SAND 87-2290.

[68] Martin J, Vitko J. ASCUAS: a solar central receiver utilizing a solid thermal carrier, Sandia National Laboratories, SAND 82-8203; 1982.
https://doi.org/10.2172/5663779

[69] Falcone PK, Noring J, Hruby J. Assessment of a solid particle receiver for a high temperature solar central receiver system. Livermore, CA: Sandia National Laboratories; 1985 (SAND 85-8208).
https://doi.org/10.2172/6023191

[70] Tan Taide, Chen Yitung. Review of study on solid particle solar receivers. Renewable and Sustainable Energy Reviews 14 (2010) 265-276.
https://doi.org/10.1016/j.rser.2009.05.012

[71] Benoit H., Pe'rez Lo'pez I., Gauthier D., Sans J.-L., Flamant G., On-sun demonstration of a 750 °C heat transfer fluid for concentrating solar systems: Dense particle suspension in tube. Solar Energy 118 (2015) 622-633.
https://doi.org/10.1016/j.solener.2015.06.007

[72] Fuliang Niea, Zhiying Cuia, Fengwu Baia, Zhifeng Wang. Properties of solid particles as heat transfer fluid in a gravity driven moving bed solar receiver. Solar Energy Materials and Solar Cells 200 (2019) 110007.
https://doi.org/10.1016/j.solmat.2019.110007

[73] Ho Clifford K., Carlson Matthew, Albrecht Kevin J., Ma Zhiwen, Jeter Sheldon, Nguyen Clayton M. Evaluation of Alternative Designs for a High Temperature Particle-to-sCO2 Heat Exchanger. Journal of Solar Energy Engineering Vol. 141 (2019).
https://doi.org/10.1115/ES2018-7504

[74] Ho Clifford K. Advances in central receivers for concentrating solar applications. Solar Energy. Volume 152 (2017) 38-56.
https://doi.org/10.1016/j.solener.2017.03.048

[75] Daniel C. Miller, Christopher J. Pfutzner, Gregory S. Jackson. Heat transfer in counterflow fluidized bed of oxide particles for thermal energy storage. International Journal of Heat and Mass Transfer 126 (2018) 730-745.
https://doi.org/10.1016/j.ijheatmasstransfer.2018.05.165

[76] Zhang S. and Wang Z., Experimental and Numerical Investigations on the Fluidized Heat Absorption inside Quartz Glass and Metal Tubes. Energies 2019, 12, 806;
https://doi.org/10.3390/en12050806

[77] Ho Clifford K., Iverson Brian D. Review of high-temperature central receiver designs for concentrating solar power. Renewable and Sustainable Energy Reviews 29 (2014) 835-846.
https://doi.org/10.1016/j.rser.2013.08.099

[78] Ávila-Marín A. L., Volumetric receivers in solar thermal power plants with central receiver system technology: A review. Solar Energy 85 (2011) 891-910.
https://doi.org/10.1016/j.solener.2011.02.002

[79] Sharma P., Chandra L., Ghoshdastidar P.S., Shekhar R. A novel approach for modelling fluid flow and heat transfer in an open volumetric air receiver using ANSYS-FLUENTP. Solar energy 204 (2020) 246-255.
https://doi.org/10.1016/j.solener.2020.04.031

[80] Singh G., Luque S., González-Aguilar J., Romero M., Chandra L., Open Volumetric Air Receiver: Current Status, Challenges and Innovative Solutions. Encyclopedia of Renewable and Sustainable Materials. Volume 1, 2020, Pages 586-599.
https://doi.org/10.1016/B978-0-12-803581-8.11263-9

[81] Miller F., Koenigsdorff R., Thermal modeling of a small-particle solar central receiver. Journal of Solar Energy Engineering-Transactions of the ASME 2000; 122 (1):23-9.
https://doi.org/10.1115/1.556277

[82] Jin Y, Fang J, Wei Jinjia, Wang X., A comprehensive model of a cavity receiver to achieve uniform heat flux using air-carbon particles mixture. Applied Energy Volume 220 (2018) 616-628.
https://doi.org/10.1016/j.apenergy.2018.03.142

[83] Ophoff C., Ozalp N., Moens D., A numerical study on particle tracking and heat transfer enhancement in a solar cavity receiver. Applied Thermal Engineering Volume 180 (2020) 115785.
https://doi.org/10.1016/j.applthermaleng.2020.115785

[84] Heller P, Pfander M, Denk T, Tellez F, Valverde A, Fernandez J, et al. Test and evaluation of a solar powered gas turbine system. Solar Energy 2006; 80 (10):1225-1230.
https://doi.org/10.1016/j.solener.2005.04.020

[85] Chu Shunzhou, Bai Fengwu, Zhang Xiliang, Yang Bei, Cui Zhiying, Nie Fuliang . Experimental study and thermal analysis of a tubular pressurized air receiver. Renewable Energy Volume 125, (2018) 413-424.
https://doi.org/10.1016/j.renene.2018.02.125

[86] Conroy T., Collins M. N., Grimes R., A review of steady-state thermal and mechanical modelling on tubular solar receivers. Renewable and Sustainable Energy Reviews 119 (2020) 109591.
https://doi.org/10.1016/j.rser.2019.109591

[87] Jorgensen G., Schissel P., Burrows R., Optical properties of high-temperature materials for direct absorption receivers. Solar Energy Materials 1986; 14 (3):385-94.
https://doi.org/10.1016/0165-1633(86)90061-4

[88] Bohn M. S., Green H. J., Heat transfer in molten salt direct absorption receivers Solar Energy, Volume 42, Issue 1, 1989, Pages 57-66.
https://doi.org/10.1016/0038-092X(89)90130-8

[89] Zhou Y., Yu J., Gao M., An experimental study of falling film evaporation in vertical channels with perforated fins of a plate-fin heat exchanger. Chemical Engineering and Processing - Process Intensification. Volume 145 (2019) 107672.
https://doi.org/10.1016/j.cep.2019.107672

[90] Tracey T. Potential of modular internal film receivers in molten salt central receiver solar power systems. In: ASME international solar energy conference, Maui, HI; April 5-9, 1992.

[91] Tyner C. E., Sutherland J. P., Gould W. R. Solar Two: A Molten Salt Power Tower Demonstration. SAND 95 - 1828 C. 1995, USA.

[92] Zheng M., Zapata J., Asselineau C-A., Coventry J., Pye J., Analysis of tubular receivers for concentrating solar tower systems with a range of working fluids, in exergy-optimised flow-path configurations. Solar Energy, Volume 211(2020) 999-1016.
https://doi.org/10.1016/j.solener.2020.09.037

[93] Robert W. Bradshaw, Daniel B. Dawson, Wilfredo De la Rosa, Rockwell Gilbert, Steven H. Goods et al. Final Test and Evaluation Results from the Solar Two Project. James E. Pacheco, Editor, Sandia National Laboratories (SAND 2002-0120).
https://doi.org/10.2172/793226

[94] Loni R., Kasaeian A.B., Mahian O., Sahin A.Z., Thermodynamic analysis of an organic Rankine cycle using a tubular solar cavity receiver. Energy Conversion and Management. Vol. 127, (2016) 494-503.
https://doi.org/10.1016/j.enconman.2016.09.007

[95] Rodríguez-Sáncheza M.R., Sánchez-González A., Marugán-Cruz C., Santana D., New designs of molten-salt tubular-receiver for solar power tower. Energy Procedia 49 (2014) 504 - 513.
https://doi.org/10.1016/j.egypro.2014.03.054

[96] Ho C. K. and Iverson B. D. Review of Central Receiver Designs for High-Temperature Power Cycles. SolarPACES 2012, Marrakech, Morocco, September 11-14, 2012.

[97] Siebers DL, Kraabel JS. Estimating convective energy losses from solar central receivers. Sandia National Laboratories, Livermore, CA. 1984. SAND 84-8717.
https://doi.org/10.2172/6906848

[98] Lu J and Ding J. Heat Transfer Performances and Exergetic Optimization for Solar Heat Receiver, Evaporation, Condensation and Heat transfer, Dr. Amimul Ahsan (Ed.), ISBN: 978-953-307-583-9, InTech (2011).
https://doi.org/10.5772/20135

[99] Clausing AM. An analysis of convective losses from cavity solar central receiver. Solar Energy 27 (1981), 295-300.
https://doi.org/10.1016/0038-092X(81)90062-1

[100] Clausing AM. Convective losses from cavity solar receivers - comparisons between analytical predictions and experimental results. Journal of Solar Energy Engineering 105, (1983) 29-33.
https://doi.org/10.1115/1.3266342

[101] Behnia M, Reizes JA, De Vahl Davis G. Combined radiation and natural convection natural-convection in a rectangular cavity with a transparent wall and containing a non-participating fluid. International Journal for Numerical Methods in Fluids, 1990, 10 (3), 305-325.
https://doi.org/10.1002/fld.1650100306

[102] Taumoefolau T, Paitoonsurikarn S, Hughes G, Lovegrove K. Experimental investigation of natural convection heat loss from a model solar concentrator cavity receiver. Journal of Solar Energy Engineering, 2004. 126 (2), 801-807.
https://doi.org/10.1115/1.1687403

[103] Sendhil Kumara, N., Reddy, K.S., 2007. Numerical investigation of natural convection heat loss in modified cavity receiver for fuzzy focal solar dish concentrator. Solar Energy 81 (7), 846-855.
https://doi.org/10.1016/j.solener.2006.11.008

[104] Prakash, M., Kedare, S.B., Nayak, J.K., 2009. Investigations on heat losses from a solar cavity receiver. Solar Energy 83, 157-170.
https://doi.org/10.1016/j.solener.2008.07.011

[105] Kistler, BL. A user's manual for DELSOL3: A computer code for calculating the optical performance and optimal system design for solar thermal central receiver plants. Sandia report, SAND 86-8018 (1986).
https://doi.org/10.2172/7228886

[106] Reynolds, D.J., Jance, M.J., Behnia, M., Morrison, G.L., 2004. An experimental and computational study of the heat loss characteristics of a trapezoidal cavity absorber. Solar Energy 76 (1-3), 229-234.
https://doi.org/10.1016/j.solener.2003.01.001

[107] Paitoonsurikarn, S., Lovegrove, K., 2006. A new correlation for predicting the free convection loss from solar dish concentrating receivers. In: Proceedings of 44th ANZSES Conference, Australia.

[108] Hazmoune M., Aour B., Chesneau X., Debbache M., Ciupageanu D. A., Lazaroiu G., Mondji Hadjiat M., Hamidat

A., Numerical Analysis of a Solar Tower Receiver Novel Design Sustainability 2020, 12, 6957.
https://doi.org/10.3390/su12176957

[109] Wu Shuangying, Xiao Lan, Cao Yiding, Li Yourong. 2010. Convection heat loss from cavity receiver in parabolic dish solar thermal power system: a review. Solar Energy 84 (8), 1342-1355.
https://doi.org/10.1016/j.solener.2010.04.008

[110] Facão J, Varga S, Oliveira AC. Evaluation of the use of artificial neural networks for the simulation of hybrid solar collectors, International Journal of Green Energy, Vol. 1, No. 3, 2004, pp. 337 - 352.
https://doi.org/10.1081/GE-200033649

[111] Benazzouz D, Benammar S, Adjerid S. Fault Detection and Isolation Based on Neural Networks Case Study: Steam Turbine. Energy and Power Engineering, 2011, 3, 513-516.
https://doi.org/10.4236/epe.2011.34062

[112] Esen H, Ozgen F, Esen M, Sengur A. Artificial neural network and wavelet neural network approaches for modelling of a solar air heater, Exp. Syst. Appl. 36 (8) (2009) 1240-11248.
https://doi.org/10.1016/j.eswa.2009.02.073

[113] Chaouachi A, Kamel R M, Ichikawa R, Hayashi H, Nagasaka K. "Neural Network Ensemble-based Solar Power Generation Short-Term Forecasting" World Academy of Science, Engineering and Technology 54 2009.

[114] Mellit A., Pavan A. M. « A 24-h forecast of solar irradiance using artificial neural network: Application for performance prediction of a grid-connected PV plant at Trieste, Italy" Solar Energy 84 (2010) 807-821.
https://doi.org/10.1016/j.solener.2010.02.006

[115] Kalogirou SA. Solar thermal collectors and applications, Progress in Energy and Combustion Science 30 (2004)
https://doi.org/10.1016/j.pecs.2004.02.001

[116] Martin J, Vitko J. ASCUAS: a solar central receiver utilizing a solid thermal carrier, Sandia National Laboratories, SAND 82-8203; 1982.
https://doi.org/10.2172/5663779

[117] Caner M, Gedik E, Kecebas A. Investigation on thermal performance calculation of two type solar air collectors using artificial neural network, Exp. Syst. Appl., 2011, 38, 1668-1674.
https://doi.org/10.1016/j.eswa.2010.07.090

[118] Benammar S., Mohammedi K., Khellaf A. Prediction of the Central Cavity Receiver's Performance Using Artificial Neural Network. 1st International Conference on Applied Automation and Industrial Diagnostics (ICAADI' 2015), DJELFA, Algeria from 29 to 30 Mars 2015.

[119] Pfahl, A. and Uhlemann, H. (2011) 'Wind loads on heliostats and photovoltaic trackers at various Reynolds numbers', J. Wind Eng. Ind. Aerodyn., Vol. 99, No. 9, pp.964-968.
https://doi.org/10.1016/j.jweia.2011.06.009

[120] Al-Rabghi, O.M. and Elsayed, M.M. (1991) 'Heliostat minimum radial spacing for no blocking and shadowing condition', Renewable Energy, Vol. 1, No. 1, pp.37-47.
https://doi.org/10.1016/0960-1481(91)90101-T

[121] Siala, F.M.F. and Elayeb, M.E. (2001) 'Mathematical formulation of a graphical method for a no-blocking heliostat field layout', Renewable Energy, Vol. 23, No. 1, pp.77-92.
https://doi.org/10.1016/S0960-1481(00)00159-2

[122] Sanchez, M. and Romero, M. (2006) 'Methodology for generation of heliostat field layout in central receiver systems based on yearly normalized energy surfaces', Solar Energy, Vol. 80, No. 7, pp.861-874.
https://doi.org/10.1016/j.solener.2005.05.014

[123] Collado, F.J. (2009) 'Preliminary design of surrounding heliostat fields', Renewable Energy, Vol. 34, No. 5, pp.1359-1363.
https://doi.org/10.1016/j.renene.2008.09.003

[124] Pitz-Paal, R., Botero, N.B. and Steinfeld, A. (2011) 'Heliostat field layout optimization for high-temperature solar thermochemical processing', Solar Energy, Vol. 85, No. 2, pp.334-343.
https://doi.org/10.1016/j.solener.2010.11.018

[125] Collado, F.J. and Guallar, J. (2012) 'Campo: generation of regular heliostat fields', Renewable Energy, Vol. 46, pp.49-59.
https://doi.org/10.1016/j.renene.2012.03.011

[126] Noone C. J., Torrilhon M., Mitsos A. Heliostat field optimization: A new computationally efficient model and biomimetic layout. Solar Energy. Volume 86, Issue 2, February 2012, Pages 792-803.
https://doi.org/10.1016/j.solener.2011.12.007

[127] Cruz N.C., Salhi S., Redondo J. L., Álvarez J. D., Berenguel M., Ortigosa P.M. Hector, a new methodology for continuous and pattern-free heliostat field optimization. Applied Energy. Volume 225, 1 September 2018, Pages 1123-1131.
https://doi.org/10.1016/j.apenergy.2018.05.072

[128] Peglow, S.G. (1979) Wind Tunnel Study of a Full-Scale Heliostat, Tech. Rep. SAND79-8034, Sandia National Laboratories, Livermore, CA.
https://doi.org/10.2172/6241465

[129] Peterka, J.A. and Derickson, R.G. (1992) Wind Load Design Methods for Ground-Based Heliostats and Parabolic Dish Collectors, Tech. Rep. SAND92-7009, Sandia National Laboratories, Albuquerque, NM.
https://doi.org/10.2172/7105290

[130] Peterka, J.A., Tan, Z., Cermak, J. and Bienkiewicz, N. (1989) 'Mean and peak wind loads on heliostats', Journal of Solar Energy Engineering, Vol. 111, No. 2, pp.158-164.
https://doi.org/10.1115/1.3268302

[131] Pfahl, A. and Uhlemann, H. (2011) 'Wind loads on heliostats and photovoltaic trackers at various Reynolds numbers', J. Wind Eng. Ind. Aerodyn., Vol. 99, No. 9, pp.964-968.
https://doi.org/10.1016/j.jweia.2011.06.009

[132] Gong B., Li Z., Wang Z., Wang Y. Wind-induced dynamic response of Heliostat. Renewable Energy Volume 38, Issue 1, February 2012, Pages 206-213.
https://doi.org/10.1016/j.renene.2011.07.025

[133] Zang CC, Christian JM, Yuan JK, Sment J, Moya AC, Ho C.K., Wang Z.F. Numerical simulation of wind loads and wind induced dynamic response of heliostats. Energy Procedia. Volume 49, 2014, Pages 1582-1591.
https://doi.org/10.1016/j.egypro.2014.03.167

[134] Vásquez-Arango JF, Buck R, Pitz-Paal R. Dynamic Properties of a Heliostat Structure Determined by Numerical and Experimental Modal Analysis. Journal of Solar Energy Engineering. Oct 2015, 137(5): 051001 (5 pages).
https://doi.org/10.1115/1.4030846

[135] Poulain P.E., Craig K.J., Meyer, J P. Variation of the height of centerline of a heliostat and influence on the wind loading. 3rd Southern African Solar Energy Conference, South Africa, 11-13 May, 2015.

[136] Zang, C., Wang, Z., Liu, X., Zhang, X. and Wang, Y. (2007) 'Design and analysis of heliostat support structure', Proceedings of ISES World Congress, Vols. 1-5.

[137] Thalange V C., Dalvi V H., Mahajani S M., Panse S V., Joshi J B, Patil R N. Design, optimization and optical performance study of tripod heliostat for solar power tower plant. Energy. Volume 135, 15 September 2017, Pages 610-624.
https://doi.org/10.1016/j.energy.2017.06.116

[138] Griffith D T, Moya A C, Ho C K, Hunter P S. Structural Dynamics Testing and Analysis for Design Evaluation and Monitoring of Heliostats. Energy Sustainability. 2011-54222, pp. 567-576.
https://doi.org/10.1115/ES2011-54222

[139] Blackmon, J.B., 2014. Heliostat drive unit design considerations - site wind load effects on projected fatigue life and safety factor. Sol. Energy, vol. 105, pp. 170-180.
https://doi.org/10.1016/j.solener.2014.02.045

[140] Modi, A., Haglind, F. Performance analysis of a Kalina cycle for a central receiver solar thermal power plant with direct steam generation. Applied Thermal Engineering, 2014, 65 201-208.
https://doi.org/10.1016/j.applthermaleng.2014.01.010

[141] Ho, CK and Kolb, GJ. Incorporating Uncertainty Into Probabilistic Performance Models of Concentrating Solar Power Plants. Journal of Solar Energy Engineering, 2010, Vol. 132 / 031012.
https://doi.org/10.1115/ES2009-90034

Received on 2-12-2020 Accepted on 27-12-2020 Published on 31-12-2020

DOI: http://dx.doi.org/10.31875/2410-2199.2020.07.9